

measured twice before the treatment and 7 times after the therapy. None of these decreased significantly with the therapy (Table 3).

Throughout the therapy, the patient exhibited chronic diarrhea that seemed to be a side effect of the treatment.

3.4. Patient 4 (myopathic form of the mtDNA depletion syndrome)

The short-term efficacy of pyruvate therapy for this female patient and her clinical and biochemical profile have been reported in detail elsewhere [3]. Briefly, the patient developed severe generalized weakness including facial muscles and respiratory failure during the neonatal period. The patient had a tracheostomy and was on a respirator. She had lactic acidosis (3.0 mM to 6.5 mM) with high lactate/pyruvate ratio (36 to 97). Muscle biopsy revealed ragged red fibers and decreased cytochrome c oxidase staining. The activities of complex I, III and IV relative to the activity of citrate synthase in the muscle were 10.6%, 26.7% and 14.1% of the control, respectively. Those relative to the activity of complex II were 6.5%, 16.4% and 8.8%, respectively. Quantitative analysis of the mtDNA revealed that the copy number of the mitochondrial ND1 subunit relative to the nuclear CFTR gene was 35.3% (normal: >40%). Exome sequencing is under way to detect a mutation in causative genes. The clinical signs and symptoms were compatible with Morava et al.'s criteria for definite mitochondrial disease [9]. As reported elsewhere, after 2 months of pyruvate therapy, the patient exhibited a mild improvement in the movement of her extremities at the age of 1 year and 9 months [3]. The overall NPMDS scores decreased from 35 to 31, but this decrease was limited to section IV. As the patient was not assessed with the GMFM, we were unable to semi-quantitatively demonstrate the improvement in motor function. One month later (after 3 months of treatment), the patient developed status epilepticus. An MRI revealed lesions in the occipital areas, which indicated a progression from the myopathic form to the encephalomyopathic form. At 5 years of age, after 41 months of treatment, scores in all sections of the NPMDS increased, and the increase in overall NPMDS score was 33.8 points compared to the score at the 2-month treatment.

Blood lactate and lactate/pyruvate ratios measured 4 times during the 2-month pre-treatment period ranged from 2.1 mM to 2.7 mM (median, 2.3 mM), and from 14.9 to 18.7 (median, 16.9), respectively. Those measured 1, 4, 6, 8 and 13 weeks after the therapy ranged from 2.3 mM to 2.7 mM (median, 2.5 mM), and from 14.1 to 21.2 (median, 17.3), respectively (Table 3). Plasma alanine, valine and lysine levels were measured once before the therapy and 4 and 8 weeks after the therapy. None of these decreased with the pyruvate therapy (Table 3).

4. Discussion

All 4 of the treated patients were severely disabled and bedridden. Therefore, objective and semi-quantitative assessments of the outcomes were difficult because the expected improvements were subtle. The NPMDS is a scale that was designed to specifically monitor mitochondrial disease, which results in a variety of multi-organ symptoms. Therefore, the scale encompasses all aspects of mitochondrial disease. Consequently, this scale cannot detect small changes in motor function. The logic applies to the JMDRS. In contrast, the GMFM-88 evaluates motor function with as many as 88 items; therefore, this assessment may detect small changes in motor abilities. However, the GMFM was designed to assess cerebral palsy, and its reliability in monitoring mitochondrial disease has not been validated. In contrast to the GMFM-66, which can only be used for cerebral palsy, the GMFM-88 has been validated for the monitoring of motor functions in disorders other than cerebral palsy, such as spinal muscular atrophy, Down syndrome and traumatic brain injuries. [10–12] Therefore, we assumed that the GMFM-88 could also be used to monitor motor functions in mitochondrial disease. Nevertheless, given that the GMFM-88 has not been validated for using in mitochondrial disease, we assessed the outcomes via a combination of the GMFM-88 and NPMDS scores with the

exception of patient 4, who was assessed only with the NPMDS. We also tried using other scales including Pediatric Evaluation of Disability Inventory (PEDI) [13] and Functional Independence Measure for Children (Wee-FIM) [14]. Our preliminary study, however, showed that these could not detect clinical changes in our patients.

Patients 3 and 4 were assessed with 2 different sets of age-specific NPMDSs as they matured into ages suitable for the application of the older age-specific NPMDSs during the monitoring period. The number of items scored in each section of the NPMDS for 2–11-year-olds is greater than that of the NPMDS for 0–24-month-olds. Therefore, it is possible that total NPMDS scores may increase when the version for older patients is used even if clinical severity remains unchanged. In Patient 3, the score for section II as assessed 2 years and 8 months decreased compared to the score assessed at 1 year and 10 months, whereas the scores for the other sections remained unchanged. Thus, a “pseudo-increase” in the score due to the use of a different set of NPMDS scales did not occur in this patient. In Patient 4, the scores for sections I, II and III increased by 8, 9 and 19 points, respectively, at 5 years of age compared to the scores observed at 21 months of age. Given that the maximum scores for sections I, II and III are higher by 6, 3 and 6 points, respectively, in the NPMDS for 2–11 year-olds than in the NPMDS for 0–24 month-olds, the increases in the scores that were higher than the maximum possible increases due to the differences in the versions of the NPMDS indicated that the increases were real.

The most noteworthy result of this study was that 3 of the 4 severely disabled patients (Patients 1, 3 and 4) exhibited improvement within 1 to 2 months of the initiation of pyruvate therapy. These improvements were confirmed by both the NPMDS and GMFM-88 (Patients 1 and 3) or the NPMDS only (Patient 4). The semi-quantitative improvement observed in Patient 4 was limited to section IV of the NPMDS, which accounts for the parents' subjective assessments. However, a descriptive observation record also revealed improvement in muscle power. [3] Given that no improvements were observed prior to pyruvate therapy in these patients and that the improvements were observed with 1–2 months of the initiation of pyruvate therapy, it is unlikely that the observed ameliorations were simply due to natural motor development rather than the effects of the therapy. The efficacy was particularly evident in Patient 1 who had m.8993 T>G and exhibited improvements in motor function that were maintained for over 2 years. The worsening of symptoms during pyruvate withdrawal also supported the efficacy of pyruvate treatment in this patient. In contrast, 2 of the 3 responsive patients did not maintain the improvements for longer than several months. Notably however, the overall NPMDS score for Patient 3 decreased (i.e., symptoms improved) after 12 months of therapy compared to this patient's score after 2 months of the therapy despite the worsening of the GMFM score. These findings indicated that the patient's overall health improved during long-term therapy, although this patient's motor abilities regressed. In Patient 4, the disease progression overwhelmed the effect of the pyruvate therapy shortly after the responsiveness was confirmed after 2 months of therapy; this finding indicated a limitation of this therapy. We could not explain why Patient 2, who had m.9176 T>C, did not respond to pyruvate therapy. Given the age of this patient, the mild improvements in motor function after 12 months of pyruvate therapy, which could not be detected with the JMDRS, seemed to be due to natural motor development rather than resulting from the treatment.

The only adverse effect of pyruvate therapy was the mild but chronic diarrhea that was observed in one patient who was on 1.0 g/kg/day of sodium pyruvate.

An *in vitro* study that utilized cybrid cells harboring MELAS m.3243A>G mutant mitochondria found that pyruvate treatment facilitates the pyruvate-to-lactate conversion, decreases the lactate/pyruvate ratio, normalizes the NADH/NAD⁺ ratio, and enhances ATP production and energy charge without significantly altering the intracellular lactate level. [15] These data support the theory that the effects of pyruvate

therapy are mediated via the normalization of the NADH/NAD⁺ ratio, which provides the NAD⁺ that is deficient in OXPHOS disturbances. In contrast to the theory and the result of this *in vitro* study, none of our responsive patients exhibited decreases in blood lactate/pyruvate ratios, which are equivalent to the NADH/NAD⁺ ratios, during the effective short-term therapy. Blood lactate levels decreased in 2 patients, especially in Patient 1, but the differences were non-significant. Thus, the blood lactate/pyruvate ratios and blood lactate levels of our patients could not be used as biochemical markers to monitor the effects of the therapy. The discrepancy between the clinical data from our patients and the *in vitro* data may be partly explained by the fact that blood lactate levels vary depending on the physical activity of the patient at the time of blood sampling, the interval between meal and sampling, as well as on the time required for the blood sampling procedure. However, all of our patients were bedridden and the data were from multiple samplings in different days. The blood samplings were done either after overnight-fast or several hours after a meal. Therefore, it is unlikely that the discrepancy was artifactual. Still, monitoring the lactate levels and lactate/pyruvate ratios in the CSF rather than in the blood would further reduce the possible artifact. Komaki et al. treated an ambulatory patient with Leigh syndrome associated with cytochrome *c* oxidase deficiency [2]. With pyruvate therapy, blood lactate level and lactate/pyruvate ratio decreased from 2.3 mM to 1.1 mM, and from 17.7 to 11.4, respectively. However, the measurements were done only once before and after the therapy, so the statistical significance could not be evaluated. Koga et al. found statistically significant decreases in blood lactate, pyruvate and alanine levels with pyruvate therapy in a non-ambulatory patient with pyruvate dehydrogenase (PDH) deficiency [4]. Blood lactate/pyruvate ratio in this patient also decreased, but the difference was non-significant (the ratios in PDH deficiency are generally normal). Differences between Komaki et al. and Koga et al.'s patients from ours were that 1) Komaki et al.'s patient was ambulatory, and 2) the pre-treatment blood levels of lactate and alanine in Koga et al.'s patient were much higher than those in our patients: the blood lactate and alanine levels in this patient were 9.6 ± 0.54 mM ($n = 8$) and 1700 ± 280 μ M ($n = 8$), respectively, while the median values of pre-treatment lactate levels in our 4 patients ranged from 1.2 to 3.9 mM and those of alanine were from 256 to 543 μ M. This may indicate that the blood lactate and alanine levels and lactate/pyruvate ratio are not sensitive biochemical markers to monitor the pyruvate therapy unless the patients are ambulatory or their pre-treatment blood levels of lactate and alanine are very high.

If the blood lactate/pyruvate ratio does not necessarily reflect the intracellular NADH/NAD⁺ ratio, the identification of a marker other than blood lactate and pyruvate is crucial. Kami et al. found that the lysine and valine levels in media in which MELAS-mutant cybrid cells were incubated with 10 mM lactate were higher than those of controls. These increases may be because catabolisms of lysine to acetyl CoA and valine to succinyl CoA require NAD⁺, which is deficient due to the imbalance in the NADH/NAD⁺ ratio [15]. Plasma levels of lysine and valine in our patients, however, did not decrease with the therapy. We do not know if the levels of these amino acids may decrease with pyruvate therapy in patients with very high blood lactate levels: Koga et al. did not measure valine and lysine levels in their responsive patient [4]. Fibroblast growth factor 21 (FGF-21), a circulating hormone-like cytokine, is reported to be one of the best biomarker with high sensitivity and specificity for detecting muscle-manifesting mitochondrial respiratory chain deficiencies [16]. Although FGF-21 has higher sensitivity than lactate or lactate/pyruvate ratio to diagnose mitochondrial disease, its utility in monitoring the disease is unknown. Further study is necessary to find biomarkers to monitor the effect of pyruvate therapy biochemically.

In conclusion, as confirmed by the GMFM-88 and/or NPMDs, pyruvate therapy was safe and effective even in severely disabled patients with OXPHOS disorders, at least in the short-term. Further studies utilizing greater numbers of patients with less severe disabilities are necessary to evaluate the long-term efficacy of this treatment. The blood lactate and pyruvate levels did not correlate with the efficacy of the

pyruvate therapy in our patients as has been reported in *in vitro* studies. The identification of more sensitive biomarkers that reflect the intracellular NADH/NAD⁺ ratio or improvements in ATP production is crucial for monitoring the clinical and biochemical efficacy of this therapy.

Conflict of interest

The authors have no conflicts of interest to disclose.

Acknowledgments

This work was supported in part by the following grants: Grants-in-Aid for Scientific Research (A-22240072, B-21390459 and C-21590411 to MT) and a Grant-in-Aid for the Global COE (Sport Sciences for the Promotion of Active Life to Waseda University) from the Ministry of Education, Culture, Sports, Science, and Technology (to MT); grants for scientific research from The Takeda Science Foundation (to MT); Grants-in-Aid for Research on Intractable Diseases (Mitochondrial Disease) (H23-016 and H23-119 to MT; H24-005 to YK, MT and TF) from the Ministry of Health, Labor and Welfare (MHLW) of Japan; and Kawano Masanori Memorial Public Interest Incorporated Foundation for Promotion of Pediatrics (to KM).

References

- [1] M. Tanaka, Y. Nishigaki, N. Fuku, T. Ibi, K. Sabashi, Y. Koga, Therapeutic potential of pyruvate therapy for mitochondrial diseases, *Mitochondrion* 7 (2007) 399–401.
- [2] H. Komaki, Y. Nishigaki, N. Fuku, H. Hosoya, K. Murayama, A. Ohtake, Y. Goto, H. Wakamoto, Y. Koga, M. Tanaka, Pyruvate therapy for Leigh syndrome due to cytochrome *c* oxidase deficiency, *Biochim. Biophys. Acta* 1800 (2010) 313–315.
- [3] K. Saito, N. Kimura, N. Oda, H. Shimomura, T. Kumada, T. Miyajima, K. Murayama, M. Tanaka, T. Fujii, Pyruvate therapy for mitochondrial DNA depletion syndrome, *Biochim. Biophys. Acta* 1820 (2012) 632–636.
- [4] Y. Koga, N. Povalko, K. Katayama, N. Kakimoto, T. Matsuishi, E. Naito, M. Tanaka, Beneficial effect of pyruvate therapy on Leigh syndrome due to a novel mutation in PDH E1 α gene, *Brain Dev.* 34 (2012) 87–91.
- [5] C. Phoenix, A.M. Schaefer, J.L. Elson, E. Morava, M. Bugiani, G. Uziel, J.A. Smeitink, D.M. Turnbull, R. McFarland, A scale to monitor progression and treatment of mitochondrial disease in children, *Neuromuscul. Disord.* 16 (2006) 814–820.
- [6] M. Alotaibi, T. Long, E. Kennedy, S. Bavishi, The efficacy of GMFM-88 and GMFM-66 to detect changes in gross motor function in children with cerebral palsy (CP): a literature review, *Disabil. Rehabil.* 36 (2014) 617–627.
- [7] S. Yatsuga, N. Povalko, Y. Nishigaki, K. Katayama, N. Kakimoto, T. Matsuishi, T. Kakuma, Y. Koga, M.S.G.I.J. Taro Matsuoka for, MELAS: a nationwide prospective cohort study of 96 patients in Japan, *Biochim. Biophys. Acta* 1820 (2012) 619–624.
- [8] P.F. Chinnery, L.A. Bindoff, 116th ENMC international workshop: the treatment of mitochondrial disorders, 14th–16th March 2003, Netherland, *Neuromuscul. Disord.* 13 (2003) 757–764.
- [9] E. Morava, L. van den Heuvel, F. Hol, M.C. de Vries, M. Hogeveen, R.J. Rodenburg, J.A. Smeitink, Mitochondrial disease criteria: diagnostic applications in children, *Neurology* 67 (2006) 1823–1826.
- [10] M. Linder-Lucht, V. Othmer, M. Walthner, J. Vry, U. Michaelis, S. Stein, H. Weissenmayer, R. Korinthenberg, V. Mall, Gross motor function measure-traumatic brain injury study, Validation of the gross motor function measure for use in children and adolescents with traumatic brain injuries, *Pediatrics* 120 (2007) e880–e886.
- [11] L. Nelson, H. Owens, L.S. Hynan, S.T. Iannaccone, S.G. Am, The gross motor function measure is a valid and sensitive outcome measure for spinal muscular atrophy, *Neuromuscul. Disord.* 16 (2006) 374–380.
- [12] D. Russell, R. Palisano, S. Walter, P. Rosenbaum, M. Gemus, C. Gowland, B. Galuppi, M. Lane, Evaluating motor function in children with Down syndrome: validity of the GMFM, *Dev. Med. Child Neurol.* 40 (1998) 693–701.
- [13] L.V. Iyer, S.M. Haley, M.P. Watkins, H.M. Dumas, Establishing minimal clinically important differences for scores on the pediatric evaluation of disability inventory for inpatient rehabilitation, *Phys. Ther.* 83 (2003) 888–898.
- [14] M.E. Msall, K. DiGaudio, B.T. Rogers, S. LaForest, N.L. Catanzaro, J. Campbell, F. Wilczenski, L.C. Duffy, The Functional Independence Measure for Children (WeeFIM): conceptual basis and pilot use in children with developmental disabilities, *Clin. Pediatr.* 33 (1994) 421–430.
- [15] K. Kami, Y. Fujita, S. Igarashi, S. Koike, S. Sugawara, S. Ikeda, N. Sato, M. Ito, M. Tanaka, M. Tomita, T. Soga, Metabolomic profiling rationalized pyruvate efficacy in cybrid cells harboring MELAS mitochondrial DNA mutations, *Mitochondrion* 12 (2012) 644–653.
- [16] A. Suomalainen, J.M. Elo, K.H. Pietilainen, A.H. Hakonen, K. Sevastianova, M. Korpela, P. Isohanni, S.K. Marjavaara, T. Tyyni, S. Kiuru-Enari, H. Pihko, N. Darin, K. Ounap, L.A. Kluijtmans, A. Paetau, J. Buzkova, L.A. Bindoff, J. Annunen-Rasila, J. Uusimaa, A. Rissanen, H. Yki-Jarvinen, M. Hirano, M. Tulinius, J. Smeitink, H. Tyyntymaa, FGF-21 as a biomarker for muscle-manifesting mitochondrial respiratory chain deficiencies: a diagnostic study, *Lancet Neurol.* 10 (2011) 806–818.

Original article

New TRPM6 mutation and management of hypomagnesaemia with secondary hypocalcaemia

Koujyu Katayama^a, Nataliya Povalko^a, Shuichi Yatsuga^a, Junko Nishioka^a,
Tatsuyuki Kakuma^b, Toyojiro Matsuishi^a, Yasutoshi Koga^{a,*}

^a Department of Pediatrics and Child Health, Kurume University Graduate School of Medicine, Kurume, Japan

^b Department of Biostatistics, Kurume University Graduate School of Medicine, Kurume, Japan

Received 18 November 2013; received in revised form 4 June 2014; accepted 6 June 2014

Abstract

Background: TRPM6 gene mutation has been reported to cause hypomagnesemia with secondary hypocalcemia (HSH). However, the genotype–phenotype correlation for TRPM6 gene mutations has not been clarified.

Objective: To elucidate the factors underlying the severe neurological complications in HSH and evaluate the potential association between the location of TRPM6 gene mutations and clinical data of HSH.

Methods: A Japanese patient diagnosed with HSH at 10 weeks of age exhibited neurological damage and failed to thrive. Magnesium supplements were therefore started at 12 weeks of age. Mutational analysis of the TRPM6 gene was performed using a direct sequencing method to determine the position and type of mutation. Using the data of 29 HSH patients reported in the literature, linear regression analysis was also performed to examine the association between TRPM6 gene mutation location and HSH onset age, initial serum magnesium and calcium concentrations, and dose of oral magnesium.

Results: A novel stop-codon homozygous mutation [c.4190 G > A] W1397X was identified in exon 26 of the patient's TRPM6 gene. No statistical correlation was found between the location of mutations in the TRPM6 gene and the clinical data for 4 clinical indicators of HSH.

Conclusions: We identified the first Japanese HSH patient with a novel nonsense mutation in the TRPM6 gene. Regression analysis of mutation locations in the protein-coding region of TRPM6 and the reported clinical data for 4 clinical indicators of HSH in 30 HSH patients did not detect a genotype–phenotype correlation.

© 2014 The Japanese Society of Child Neurology. Published by Elsevier B.V. All rights reserved.

Keywords: TRPM6; HSH; Genotype–phenotype correlation; Magnesium; Mental retardation; Failure to thrive

1. Introduction

Abbreviations: HSH, hypomagnesemia with secondary hypocalcemia; TRPM6, transient receptor potential channel melastatin 6

* Corresponding author. Address: Department of Pediatrics and Child Health, Kurume University School of Medicine, 67 Asahi-Machi, Kurume City, Fukuoka 830-0011, Japan. Tel.: +81 942 31 7565; fax: +81 942 38 1792.

E-mail address: yasukoga@med.kurume-u.ac.jp (Y. Koga).

Hypomagnesemia with secondary hypocalcemia (HSH, OMIM #602014) is a rare autosomal recessive disorder that is characterized by the development of neurological symptoms, including tetany, muscle spasms, and seizures, in early infancy due to low serum magnesium [1]. The low serum magnesium levels

associated with HSH result from defective intestinal magnesium absorption and increased renal magnesium clearance, which lead to secondary hypocalcemia due to insufficient secretion and resistance to parathyroid hormone (PTH) [2,3]. To help prevent the negative outcomes of PTH deficiency, which include severe neurological damage and even death, HSH patients require life-long oral magnesium supplementation [4,5]. In 2002, an association was identified between HSH and mutations in the gene encoding the transient receptor potential channel melastatin 6 (TRPM6), which is involved in transepithelial magnesium transport and belongs to the transient receptor potential (TRP) family of cation channels [6,7]. To date, at least 38 *TRPM6* mutations have been reported and include stop codon, frame-shift, and splice-site mutations, and exon deletions [4]. Although an apparent association exists between the development of HSH and *TRPM6* abnormality, no definitive genotype–phenotype correlation has been established between *TRPM6* gene mutations and disease severity [5].

2. Patient

The patient was an infant female born as the first child of consanguineous parents of Japanese origin. The patient's family pedigree is presented in Fig. 1A. The patient was delivered without problems and had a birth weight of 2795 g. At 72 days of age, the patient had a generalized tonic seizure with apnea, and was then admitted to a local hospital. Blood examination showed hypocalcemia (1.98 mmol/l; reference value: 2.2–2.7 mmol/l); however, the symptoms improved without any specific treatment after 1 week.

At 81 days of age, the patient was referred to our hospital because of recurrent seizure. On admission, the patient presented with seizure, muscle hypotonia, and severe irritability. Although blood examination showed hypocalcemia (1.55 mmol/l), the level of parathyroid hormone (PTH) was normal (17 pg/ml, reference value: 12–92 pg/ml). Blood urea nitrogen, creatinine, electrolytes, blood glucose and urinalysis were within normal ranges. Electroencephalogram and magnetic resonance imaging of the brain did not show any specific findings. Midazolam (0.2 mg/kg/h) for seizure and calcium gluconate (calcium; 35.2 mg/kg/day) for hypocalcemia were administered. After admission to our hospital, hypomagnesemia was detected (0.10 mmol/l; reference value: 0.75–1.25 mmol/l). Fractional magnesium excretion (FEMg⁺²) was 2.7% (reference value: 1.0–8.0%), indicating that the renal absorption of magnesium was impaired. For this reason, magnesium was intravenously administered (4.37–5.47 mg/kg/day) at 84 days of age. All symptoms disappeared in accordance with normalization of the serum magnesium level. Creatinine clearance and urinary electrolytes, including calcium excretion, were within normal ranges. Renal ultrasonography was normal. Based on these findings, the patient was clinically diagnosed with HSH.

At 93 days of age, the patient was orally administered magnesium (26.73 mg/kg/day) four times daily in place of intravenous magnesium treatment. After 2 days of oral magnesium, the patient had mild diarrhea and irritability due to hypomagnesemia (0.49 mmol/l). The patient's irritability was reduced by increasing the dose of oral magnesium to 53.46 mg/kg/day, and the mild diarrhea also improved following the administration of oral magnesium with probiotics six times daily. The

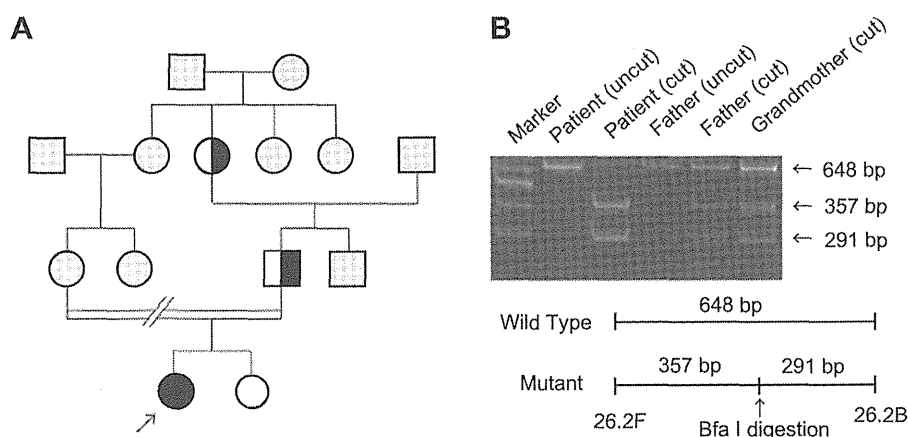


Fig. 1. Patient's family pedigree and genetic analysis of the *TRPM6* gene. (A) Patient's family tree. The parents and sister of the proband did not have symptoms of HSH. Filled symbols, study patient; open symbols, wild-type haplotype; semi-filled symbols, heterozygous mutation carriers; grey symbols, unknown genotype; female; square, male; double slash, divorce. (B) Identification of the W1397X mutation in the *TRPM6* gene. PCR-RFLP analysis was performed to identify mutations in the patient's *TRPM6* gene using SDS-PAGE separated on an 0.8% gel. The patient has a homozygous W1397X mutation in the *TRPM6* gene, and the patient's father and grandfather are heterozygous for this mutation. The restriction enzyme *Bfa*I was used in the analysis.

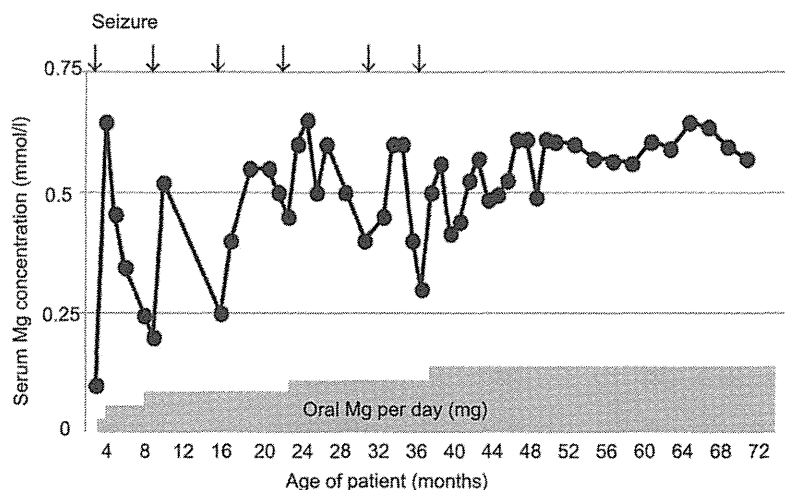


Fig. 2. Patient's clinical course. With increasing oral magnesium (Mg) administration over time, the patient's serum Mg concentration reached or exceeded the lower normal limit (0.75–1.25 mmol/l) and the number and frequency of seizures gradually decreased. Arrows indicate the occurrence of a seizure. Gray bars indicate the dose (mg/day) of orally administered Mg. The patient received a Mg dose of 101.45 mg/day at 3 months of age; 202.91 mg/day between 4 and 8 months of age; 242.40 mg/day between 8 and 24 months of age; and a maximum dose of 568.62 mg/day from 24 to 38 months of age.

patient was discharged after her serum magnesium level became stable (0.53–0.74 mmol/l) at 120 days of age. The patient's clinical course is shown in Fig. 2.

Due to poor drug compliance, the patient experienced several symptoms, including seizure, irritability, and photophobia, related to low magnesium serum levels and occasionally required intravenous infusion of magnesium until 3 years of age. The patient experienced mild diarrhea as a side effect of oral magnesium. The last reported seizure occurred at 3 years of age (Fig. 2). At 4 years of age, the patient scored 52 on an intelligence quotient test (Tanaka-Binet test) (normal > 85) and had a height of 93.0 cm (−2.7 SD for the standard height of Japanese girls). The patient was evaluated for growth hormone (GH) deficiency at 4 years and 8 months of age by performing an arginine infusion test. The patient's peak plasma GH concentration increased from 2.3 to 17.7 ng/ml after arginine infusion, suggesting that GH deficiency was not a factor.

The patient's parents provided written informed consent for the genetic analysis to be performed and for the patient's clinical data to be published. The study protocol was approved by the Ethics Committee of the Kurume University Graduate School of Medicine.

3. Methods

3.1. Mutational analysis

Extraction of DNA from white blood cells was performed using standard protocols. We designed 41 primer sets (primer sequences are available upon request) based on the sequence of the human TRPM6

gene (genomic contig GenBank accession No. NC_000009) to amplify the complete coding sequence (exons 1–39; exon 26 required 3 primer sets to cover the entire exon) and intron/exon boundaries of the TRPM6 gene from genomic DNA. Both strands of the amplified products were directly sequenced using a CEQ Dye Terminating Cycle Sequencing Kit (Beckman Coulter, Inc., Fullerton, CA) on a CEQ™ 8000 Genetic Analysis System (Beckman Coulter, Inc.). The sequences were assembled into a contig using the DNASIS Pro program (Hitachi Software Engineering Co., Ltd., Japan), and the resulting contig was aligned to the sequence of the human TRPM6 gene. To determine if the W1397X mutation was present in the patient's family members, PCR-RFLP analysis was performed using the primer set TRPP6.26.2F and TRPM6.26.2B, and the restriction endonuclease *Bfa*I.

3.2. Statistical analysis

Linear regression analysis was performed to investigate the association between the location of mutations in the TRPM6 gene and four clinical indicators of HSH: age of disease onset, initial serum magnesium and calcium concentrations (mmol/l), and dose of oral magnesium supplement (mg/kg/day) for 29 patients reported in the literature (Table 1). Patients with mutations in introns were excluded from the analysis. A total of 30 patients, which included the present study patient, were included in the analysis (Table 1) [5,6,8–12]. The level of statistical significance was set at $p > 0.05$. All analyses were performed using SPSS statistical software (SPSS Inc., Chicago, IL).

Table 1
Clinical data and *TRPM6* mutations of the 30 HSH patients analyzed in the present study.

Case	Exon	<i>TRPM6</i> mutation	Onset age (day)	Initial serum Mg/Ca (mmol/l)	Amount of oral Mg (mg/kg/day)	Refs.
1	25	Q1186X	90	0.16/1.8	4.86	[10]
2	25	Q1186X	90	0.08/1.8	9.72	[10]
3	12	R474X	16	0.32/1.78	250	[9]
4	5	E157X	35	0.16/1.43	20	[11]
5	16	S590X	60	0.21/1.63	25.03	[5,6]
6	4	S141L	120	0.1/2.50	32.81	[5,6]
7	11/ 26	H427fsX429 + 1260fsX283	35	0.41/1.88	75.35	[5,6]
8	17	R736fsX737	35	0.17/1.5	19.44	[5,8]
9	17	R736fsX737	35	0.22/1.6	18.23	[5,8]
10	32/ 33	Del exons 31 + 32	150	0.15/1.94	11.91	[5]
11	32/ 33	Del exons 31 + 32	35	0.22/1.73	10.21	[5]
12	22/ 23	Del exons 23 + 24	90	ND/1.74	9.97	[5]
13	30	L1673fsX1675	60	0.2/1.31	13.61	[5]
14	21	I944fsX959	42	ND/	13.37	[5]
15	26	Fs + preterm stp	60	0.1/1.66	72.92	[5]
16	26	Fs + preterm stp	120	0.19/	94.79	[5]
17	36	Loss of splice site/exon skipping	9	0.09/1.6	13.12	[5]
18	36	Loss of splice site/exon skipping	120	0.16/1.75	22.85	[5]
19	21	R928X	21	0.2/1.35	24.79	[5]
20	16	P599fsX609	35	0.29/1.45	42.05	[5]
21	21	Del exon 21	28	0.44/1.7	60.03	[5]
22	5	E157X	90	0.1/1.45	48.61	[5]
23	26	R1533X	60	/	17.26	[5]
24	6	D223fsX263	180	0.3/1.75		[5]
25	23	Y1053C		0.05/1.78	23.51	[12]
26	5/34	E157X + S1754 N	120	0.2/1.6	12.15	[12]
27	17	L708P + Loss of splice site	42	0.12/1.6	45.2	[12]
28	19/ 29	E872G + Q1663R	270	0.1/1.47	36.45	[12]
29	25	L1143P + Loss of splice site	60	0.08/1.94	18.23	[12]
30	26	W1397X	72	0.1/1.98	53.46	Present
Median	21.75		60.0	0.16/1.70	22.85	
Range	4–36		16–270	0.05–0.44/1.31–2.50	4.86–250	
<i>p</i> Value (vs. exon)			0.65	0.29/0.82	0.15	

Mg, magnesium; Ca, calcium; ND, not detectable; Del, deletion; Fs, frame shift.

4. Results

4.1. Mutational analysis

A novel homozygous stop-codon mutation, [c.4190 G > A] W1397X, was detected in exon 26 of the patient's *TRPM6* gene based on the results of PCR-RFLP analysis (Fig. 1B). The patient's father and paternal grandmother were heterozygous for this mutation, whereas the patient's younger sister had wild-type *TRPM6* alleles (Fig. 1A). No member of the patient's immediate family had any clinical symptoms of HSH or abnormal laboratory findings related to serum magnesium, calcium, phosphate, and intact PTH levels. Unfortunately,

the genotype of the patient's mother could not be determined as she was separated from the family due to divorce. Based on the genotype of the patient and the patient's father, the mother was likely heterozygous for the W1397X mutation. However, because no molecular analyses for chromosomal abnormalities were performed, we cannot exclude the possibility of uniparental disomy from the patient's father.

4.2. Association between *TRPM6* gene mutation location and clinical data of HSH

To investigate if a correlation exists between the degree of loss of function of the *TRPM6* protein

resulting from gene mutation and HSH severity we retrospectively analyzed the reported clinical data of 30 HSH patients, including the present study patient, with mutations in exons of the TRPM6 gene (Table 1). Linear regression analysis was performed for several clinical parameters of HSH, specifically disease onset age, initial serum magnesium and calcium concentrations, and oral magnesium dose. However, no significant correlations between the total number of exons in the TRPM6 gene and each of the four examined parameters of HSH severity were detected.

5. Discussion

We identified the first Japanese HSH patient with a novel homozygous stop-codon mutation in exon 26 of the TRPM6 gene. The patient manifested recurrent seizures at 10 weeks of age, leading to the diagnosis of HSH, and suffered from both physical and mental impairment in the form of short stature and mental retardation despite magnesium supplementation. One of the underlying causes of the complications was possibly due to poor drug compliance as a result of family problems. The retrospective analysis of 29 HSH patients with TRPM6 gene mutations did not detect a relationship between mutation location and any of the four indicators of HSH. Our findings suggest that preventing severe complications of HSH requires early diagnosis and good drug compliance to avoid recurrent seizures and permanent mental damage. In addition, clinical data for serum calcium and magnesium levels is not expected to aid in the genetic screening of nonsense mutations in the TRPM6 gene.

Our HSH patient exhibited early signs of mild mental retardation and had a low IQ test score at 4 years of age. Although HSH patients typically have normal psychomotor development, delayed diagnosis and repeated convulsions can cause mild to severe mental retardation as a result of neurological damage [4,5]. In the present patient, mental retardation may have resulted from the slightly delayed diagnosis of HSH and unstable serum magnesium levels associated with frequent diarrhea, which resulted in repeated convulsions over a 2.5-years period. In addition, family problems led to inadequate nurturing and low drug compliance, which likely contributed to the patient's low serum magnesium levels, convulsions, and mental impairment.

The patient's symptoms, particularly the frequency of seizures, gradually improved with increasing serum magnesium levels. Several additional factors may have influenced the patient's clinical improvement, including the oral administration of probiotics, avoidance of allergic foods, and improved family care. Although the mechanisms by which hypomagnesemia causes neurological damage are unknown, impaired voltage-dependent

magnesium gating of the N-methyl-D-aspartate receptor may induce seizures [13,14]. In TRPM6 knockout mice, abnormal development and neural tube defects were observed [15], suggesting that TRPM6 affects nerve development. Mental retardation has also been reported in HSH patients due to the delayed administration of magnesium [4,5]. Our patient experienced seizures when serum magnesium fell below 0.4 mmol/l as a result of poor drug compliance. Thus, the rapid diagnosis of HSH and supplementation of magnesium above a threshold serum level are important to prevent psychomotor impairment.

Our patient had short stature and failed to thrive. Although growth disorders are rarely observed in HSH patients and the underlying mechanisms remain unclear [5,14], inadequate nutrition might be a major contributing factor. It is also possible that our patient's unstable family environment impacted her development, as short stature and failure to thrive have been reported for children who have suffered from physical and mental abuse [16–19]. At the time of writing, the patient had stable serum magnesium levels, was free from family problems, and had normal GH secretion. Thus, it is possible that young HSH patients with short stature and failure to thrive may improve with continued magnesium supplementation.

Schlingmann et al. [5] first reported that no genotype–phenotype correlation exists for HSH, and since this publication, a definitive genotype–phenotype correlation has not been demonstrated for this disorder. Most of the mutations in the HSH patients included in the present analyses (Table 1) would theoretically result in nonsense-mediated decay of TRPM6 mRNA and caused reduced TRPM6 protein translation [20]. Moreover, due to the large size of the TRPM6 gene, which consists of 39 exons spanning 167 kb of genomic sequence and codes for a protein of 2022 amino acids (Fig. 3), mutational screening is time consuming and expensive. If nonsense mutations leading to protein dysfunction or rapid mRNA decay could be predicted from clinical data, it would increase the efficiency of mutational screening and detection. We speculated that the total number of exons encoding the protein may be correlated with the clinical parameters of HSH. However, our present analyses of 30 HSH patients suggest that no correlation exists between TRPM6 genotype and the clinical parameters of HSH, demonstrating that clinical data are not useful for the estimation of the exon mutation site.

Several limitations of the present study warrant mention. First, as only one HSH patient with a stop-codon mutation in exon 26 of the TRPM6 gene was analyzed, our findings need to be confirmed in other patients who also possessed the identified mutation. Second, the linear regression analysis only included the data of 30 patients, a sample size that may have been too small to

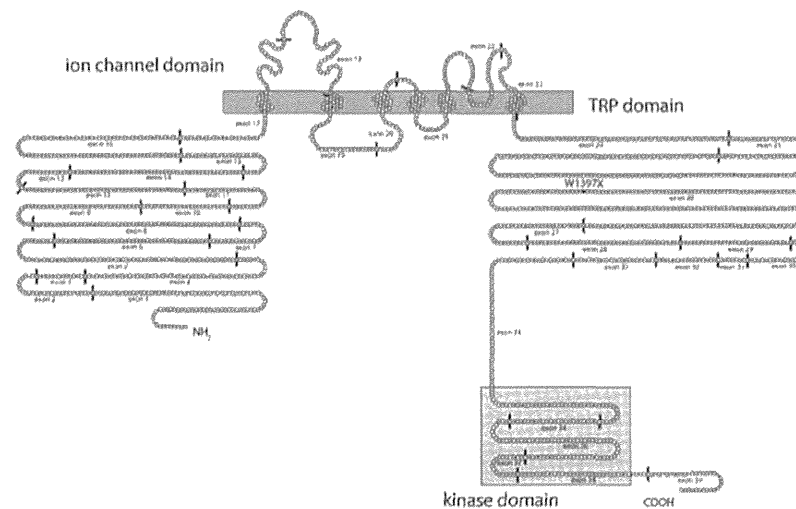


Fig. 3. Structure of the TRPM6 gene and exons. The TRPM6 gene consists of 39 exons spanning 167 kb of genomic sequence and coding for a protein of 2022 amino acids. The TRPM6 protein harbors an ion channel region with six transmembrane domains and a putative pore region between the fifth and sixth transmembrane domain, a long N-terminus conserved within the TRPM family, a TRP domain of unknown function located C-terminally of the ion channel domain, and a C-terminal kinase domain with sequence similarity to atypical α kinases. The structural organization of the TRPM6 gene presented in this figure was adapted from Ref. [20].

detect a relationship between exon number of the genetic abnormality and serum magnesium levels. Finally, the trend of increasing magnesium levels with the increasing level of TRPM6 gene impairment may have been influenced by differences in the therapeutic strategies between patients.

6. Conclusions

We describe here a Japanese HSH patient with a novel mutation in exon 26 of the TRPM6 gene. Despite the administration of magnesium at 12 weeks of age, the patient experienced family problems that may have adversely affected drug compliance, leading to short stature and mental retardation. The location analysis of mutations in the protein-coding region (exon number) of TRPM6 in 30 HSH patients and the 4 examined clinical parameters of disease showed that no genotype–phenotype correlation exists for HSH, as has been reported previously.

Acknowledgement

This work was supported in part by a grant (#16390308) from the Ministry of Culture and Education in Japan to Y.K.

Appendix A. Supplementary data

Supplementary data associated with this article can be found, in the online version, at <http://dx.doi.org/10.1016/j.braindev.2014.06.006>.

References

- [1] Paunier L, Raddle IC, Kooh SW, Conen PE, Fraser D. Primary hypomagnesemia with secondary hypocalcemia in an infant. *Pediatrics* 1968;41:385–402.
- [2] Lombeck I, Ritzl F, Schnippering HG, Michael H, Bremer HJ, Feinendegen LE, et al. Primary hypomagnesemia. I. Absorption Studies. *Z Kinderheilkd* 1975;118:249–58.
- [3] Milla PJ, Aggett PJ, Wolff OH, Harries JT. Studies in primary hypomagnesaemia: evidence for defective carrier-mediated small intestinal transport of magnesium. *Gut* 1979;20:1028–33.
- [4] Shalev H, Phillip M, Galil A, Carmi R, Landau D. Clinical presentation and outcome in primary familial hypomagnesaemia. *Arch Dis Child* 1998;78:127–30.
- [5] Schlingmann KP, Sassen MC, Weber S, Pechmann U, Kusch K, Pelken L, et al. Novel TRPM6 mutations in 21 families with primary hypomagnesemia and secondary hypocalcemia. *J Am Soc Nephrol* 2005;16:3061–9.
- [6] Schlingmann KP, Weber S, Peters M, Niemann Nejsum L, Vitzthum H, Klingel K, et al. Hypomagnesemia with secondary hypocalcemia is caused by mutations in TRPM6, a new member of the TRPM gene family. *Nat Genet* 2002;31:166–70.
- [7] Walder RY, Landau D, Meyer P, Shalev H, Tsolia M, Borochowitz Z, et al. Mutation of TRPM6 causes familial hypomagnesaemia with secondary hypocalcemia. *Nat Genet* 2002;31:171–4.
- [8] Challa A, Papaefstathiou I, Lapatsanis D, Tsolas O. Primary idiopathic hypomagnesemia in two female siblings. *Acta Paediatr* 1995;84:1075–8.
- [9] Esteban-Oliva D, Pintos-Morell G, Konrad M. Long-term follow-up of a patient with primary hypomagnesaemia and secondary hypocalcaemia due to a novel TRPM6 mutation. *Eur J Pediatr* 2009;168:439–42.
- [10] Guran T, Akcay T, Bereket A, Atay Z, Turan S, Haisch L, et al. Clinical and molecular characterization of Turkish patients with familial hypomagnesaemia: novel mutations in TRPM6 and CLDN16 genes. *Nephrol Dial Transplant* 2012;27:667–73.
- [11] Apa H, Kayserili E, Agin H, Hizarcioğlu M, Gulez P, Berdeli A. A case of hypomagnesaemia with secondary hypocalcemia caused by Trpm6 gene mutation. *Indian J Pediatr* 2008;75:632–4.

- [12] Lainez S, Scilingmann KP, van der Wijst J, Dworniczak B, van Zeeland F, Konrad M, et al. New TRPM6 missense mutations linked to hypomagnesemia with secondary hypocalcemia. *Eur J Hum Genet* 2013;1–8.
- [13] Mody I, Lambert JD, Heinemann U. Low extracellular magnesium induces epileptiform activity and spreading depression in rat hippocampal slices. *J Neurophysiol* 1987;57:869–88.
- [14] Hartnett KA, Stout AK, Rajdev S, Rosenberg PA, Reynolds IJ, Aizenman E. NMDA receptor-mediated neurotoxicity: a paradoxical requirement for extracellular Mg^{2+} in Na^+/Ca^{2+} -free solutions in rat cortical neurons in vitro. *J Neurochem* 1997;68:1836–45.
- [15] Walder RY, Yang B, Stokes JB, Kirby PA, Cao X, Shi P, et al. Mice defective in *Trpm6* show embryonic mortality and neural tube defects. *Hum Mol Genet* 2009;18:4367–75.
- [16] Cole DE, Kooh SW, Vieth R. Primary infantile hypomagnesemia: outcome after 21 years and treatment with continuous nocturnal nasogastric magnesium infusion. *Eur J Pediatr* 2000;159:38–43.
- [17] Munoz-Hoyos A, Molina-Carballo A, Augustin-Morales M, Contreras-Chova F, Naranjo-Gomez A, Justicia-Martinez F, et al. Psychosocial dwarfism: psychopathological aspects and putative neuroendocrine markers. *Psychiatry Res* 2011;188:96–101.
- [18] Japtap VS, Sarathi V, Lila AR, Bukan AP, Bandgar T, Menon P, et al. Hyperphagic short stature: a case report and review of literature. *Indian J Endocrinol Metab* 2012;16:624–6.
- [19] Skuse D, Albanese A, Stanhope R, Gilmour J, Voss L. A new stress-related syndrome of growth failure and hyperphagia in children associated with reversibility of growth-hormone insufficiency. *Lancet* 1996;348:353–8.
- [20] Scilingmann KP, Waldegger S, Konrad M, Chubanov V, Guder-mann T. TRPM6 and TRPM7—Gatekeepers of human magnesium metabolism. *Biochim Biophys Acta* 2007;1772:813–21.

AUTHOR QUERY FORM

Journal: CMET
Article Number: 1726

Dear Author,

Please check your proof carefully and mark all corrections at the appropriate place in the proof.

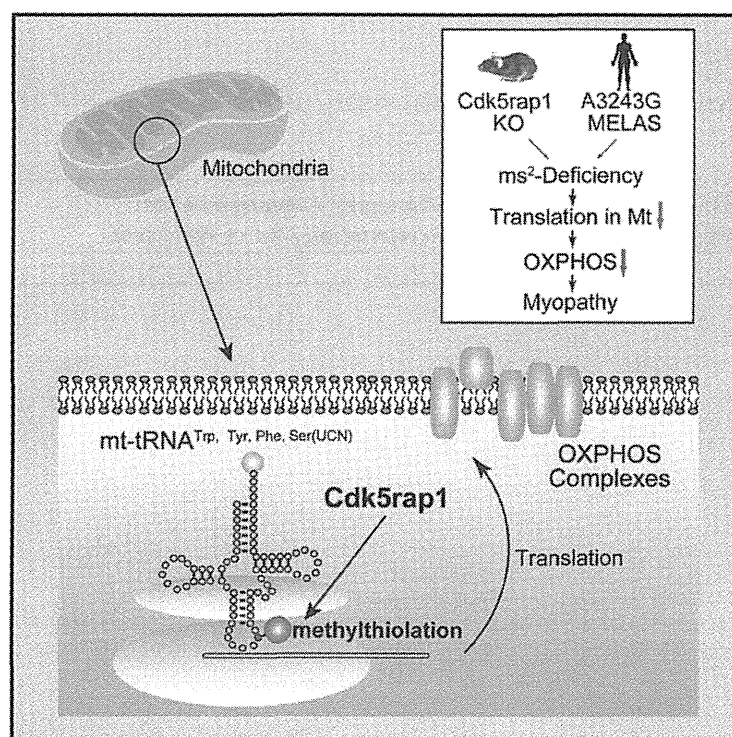
Location in article	Query / Remark: Click on the Q link to find the query's location in text Please insert your reply or correction at the corresponding line in the proof
	There are no queries in this article

Thank you for your assistance.

Cell Metabolism

Cdk5rap1-Mediated 2-Methylthio Modification of Mitochondrial tRNAs Governs Protein Translation and Contributes to Myopathy in Mice and Humans

Graphical Abstract



Authors

Fan-Yan Wei, Bo Zhou, ..., Yuichi Oike, Kazuhito Tomizawa

Correspondence

tomikt@kumamoto-u.ac.jp

In Brief

Wei et al. report that Cdk5rap1 is responsible for 2-methylthio (ms^2) modifications of mammalian mt-tRNAs. The modification is critical for efficient mitochondrial translation in mice and dysregulated in MELAS patients.

Highlights

- Cdk5rap1 catalyzes 2-methylthio (ms^2) modification of four mitochondrial tRNAs
- The ms^2 modifications optimize mitochondrial translation and OXPHOS activity
- Deficiency of ms^2 modification accelerates myopathy and cardiac dysfunction in mice
- The ms^2 modification levels are reduced in patients with mitochondrial disease

Wei et al., 2015, Cell Metabolism 21, 1–15
 March 3, 2015 ©2015 Elsevier Inc.
<http://dx.doi.org/10.1016/j.cmet.2015.01.019>

CellPress

Cdk5rap1-Mediated 2-Methylthio Modification of Mitochondrial tRNAs Governs Protein Translation and Contributes to Myopathy in Mice and Humans

Fan-Yan Wei,^{1,7} Bo Zhou,^{1,7} Takeo Suzuki,³ Keishi Miyata,² Yoshihiro Ujihara,⁴ Haruki Horiguchi,² Nozomu Takahashi,¹ Peiyu Xie,¹ Hiroyuki Michiue,⁵ Atsushi Fujimura,⁵ Taku Kaitsuka,¹ Hideki Matsui,⁵ Yasutoshi Koga,⁵ Satoshi Mohri,⁴ Tsutomu Suzuki,³ Yuichi Oike,² and Kazuhito Tomizawa^{1,*}

¹Department of Molecular Physiology

²Department of Molecular Genetics

Faculty of Life Sciences, Kumamoto University, Kumamoto 860-8556, Japan

³Department of Chemistry and Biotechnology, School of Engineering, The University of Tokyo, Tokyo 113-8656, Japan

⁴First Department of Physiology, Kawasaki Medical School, Okayama 701-0192, Japan

⁵Department of Physiology, Okayama University Graduate School of Medicine, Dentistry and Pharmaceutical Sciences, Okayama 700-8558, Japan

⁶Department of Pediatrics and Child Health, Kurume University Graduate School of Medicine, Fukuoka 830-0011, Japan

⁷Co-first author

*Correspondence: tomikt@kumamoto-u.ac.jp

<http://dx.doi.org/10.1016/j.cmet.2015.01.019>

SUMMARY

Transfer RNAs (tRNAs) contain a wide variety of post-transcriptional modifications that are important for accurate decoding. Mammalian mitochondrial tRNAs (mt-tRNAs) are modified by nuclear-encoded tRNA-modifying enzymes; however, the physiological roles of these modifications remain largely unknown. In this study, we report that Cdk5 regulatory subunit-associated protein 1 (Cdk5rap1) is responsible for 2-methylthio (ms^2) modifications of mammalian mt-tRNAs for Ser(UCN), Phe, Tyr, and Trp codons. Deficiency in ms^2 modification markedly impaired mitochondrial protein synthesis, which resulted in respiratory defects in Cdk5rap1 knockout (KO) mice. The KO mice were highly susceptible to stress-induced mitochondrial remodeling and exhibited accelerated myopathy and cardiac dysfunction under stressed conditions. Furthermore, we demonstrate that the ms^2 modifications of mt-tRNAs were sensitive to oxidative stress and were reduced in patients with mitochondrial disease. These findings highlight the fundamental role of ms^2 modifications of mt-tRNAs in mitochondrial protein synthesis and their pathological consequences in mitochondrial disease.

INTRODUCTION

Transfer RNA (tRNA) is a key molecule in the translational apparatus to decode genetic information into proteins. A unique feature of tRNAs is the presence of a variety of chemical modifications of their nucleotides (Machnicka et al., 2013). These modifications are critical for efficient and accurate decoding (Agris, 2004; Suzuki, 2005). To date, more than 100 modified nucleotides

have been identified in tRNAs from the three domains of life, indicative of the universal importance of tRNA modifications (Machnicka et al., 2013).

Given the critical roles of tRNA modifications in cells, it is not surprising that tRNA modification deficiencies have been associated with human diseases (Torres et al., 2014). Genetic variations in the gene encoding Cdk5 regulatory subunit associated protein 1-like-1 (CDKAL1), which inserts a 2-methylthio (ms^2) group into the N^6 -threonylcarbamoyl adenosine (t^6A) of cytosolic tRNA^{Lys}(UUU), have been associated with the development of type 2 diabetes (Steinthorsdottir et al., 2007; Arragain et al., 2010). A deficiency in the ms^2 modification of tRNA^{Lys}(UUU) resulted in aberrant proinsulin synthesis, which ultimately led to impaired glucose metabolism and insulin secretion in Cdkal1 knockout (KO) mice and in human subjects carrying T2D-associated alleles of *CDKAL1* (Wei et al., 2011; Xie et al., 2013).

In mitochondrial tRNAs (mt-tRNAs), 15 species of modified nucleotides at 118 positions have been identified in bovine (Suzuki and Suzuki, 2014). Some of these modifications have been associated with the development of mitochondrial diseases, such as Mitochondrial myopathy, encephalopathy, lactic acidosis, stroke-like episodes (MELAS), and myoclonus epilepsy with ragged-red fibers (MERRF) (Suzuki et al., 2011). mt-tRNA^{Leu} and mt-tRNA^{Lys} contain 5-taurinomethyl (τm^5) and 5-taurinomethyl-2-thio (τm^5s^2) modifications, respectively, at U34 (Yasukawa et al., 2001; Suzuki et al., 2002), and both of these modifications are critical for decoding their cognate codons (Kirino et al., 2004; Yasukawa et al., 2001). The absence of these modifications has been observed in MELAS patients carrying the A3243G mutation in mt-tRNA^{Leu} and in MERRF patients carrying the A8344G mutation in mt-tRNA^{Lys} (Yasukawa et al., 2001). These results suggest a critical role for mt-tRNA modifications in the pathogenesis of human diseases. Nevertheless, knowledge regarding the physiological roles of tRNA modifications is incomplete, and a complete investigation of the individual types of mt-tRNA modifications is required to fully understand the physiological function and molecular pathology of tRNA modifications in human diseases.

In mammalian mt-tRNAs, 2-methylthio-*N*⁶-isopentenyl adenosine (ms²i⁶A) is a unique modification that is conserved in all three domains of life (Machnicka et al., 2013). In bacteria, the ms² modification of ms²i⁶A contributes to accurate decoding by improving tRNA binding to codons (Urbonavicius et al., 2001; Jenner et al., 2010). However, the physiological importance of ms² modifications in mammals is unknown. We have previously shown that Cdk5rap1 might be responsible for the ms² modification of ms²i⁶A because of its homology to Cdkal1, which catalyzes ms²t⁶A modification (Arragain et al., 2010). Recently, Cdk5rap1 was proposed to catalyze ms² group insertion in both cytosolic RNAs and mt-tRNAs; however, the exact substrate tRNA of Cdk5rap1 in mammalian cells remains unclear (Reiter et al., 2012).

Given the exclusive mitochondrial localization of ms²i⁶A in mammals and the implication of this localization in the decoding process, we hypothesize that Cdk5rap1 might specifically catalyze the ms² modification of mt-tRNAs and contribute to mitochondrial function *in vivo*. In this study, we validated this hypothesis through a thorough investigation of the physiological function of the ms² modification in Cdk5rap1 KO mice. Furthermore, we investigated the pathological implication and the molecular mechanism of the ms² modification in MELAS patients.

RESULTS

Cdk5rap1 Catalyzes the Conversion of i⁶A to ms²i⁶A in Mitochondrial tRNAs

Based on the high homology between mammalian Cdk5rap1 and bacterial MiaB, we and another group previously showed that Cdk5rap1 might be a mammalian methylthiotransferase that catalyzes the conversion of *N*⁶-isopentenyl adenosine (i⁶A) to 2-methylthio-*N*⁶-isopentenyl adenosine (ms²i⁶A) (Figure 1A and see Figure S1A available online; Arragain et al., 2010; Reiter et al., 2012). To investigate this hypothesis, we transformed Cdk5rap1 in MiaB-deficient bacteria (Δ MiaB), which do not contain ms² modifications. As expected, the transformation of Cdk5rap1 restored ms² modifications (Figure 1B). The conserved cysteine residues in the UPF domain and the radical SAM domain of MiaB are critical for ms² modification through their interaction with two [4Fe-4S] clusters (Forouhar et al., 2013). Similar to MiaB, the mutation of cysteine residues in the UFP domain or the radical SAM domain of Cdk5rap1 completely abolished the ms² modification (Figure 1B).

To prove that Cdk5rap1 is a mitochondrial methylthiotransferase and to identify its exact substrates, we generated Cdk5rap1 KO mice (Figures S1B–S1D). As expected, the ms² modification was completely abolished in KO mice (Figures S1E and S1F). Cdk5rap1 colocalized with Mitotracker in HeLa cells (Figure S2A). Cdk5rap1 with a deletion of mitochondrial localization signal at the N terminus exhibited cytosolic localization but retained its enzyme activity (Figures S2A and S2B). However, no ms² modification was detected in Cdk5rap1-deficient mouse embryonic fibroblast (MEF) cells expressing the cytosolic form of Cdk5rap1 (Figures S2C and S2D). These results indicate that Cdk5rap1 localizes on mitochondria and specifically modifies mt-tRNAs. To identify the exact substrate of Cdk5rap1, individual mt-tRNA was isolated from WT and KO mice and subjected to mass spectrometric analysis. The ms² modification

was completely absent at A37 in mt-tRNA^{Phe}, mt-tRNA^{Trp}, mt-tRNA^{Tyr}, and mt-tRNA^{Ser(UCN)} isolated from KO mice (Figures 1C–1F). The absence of an ms² modification did not affect the nearby γ m⁵ modification at U34 in mt-tRNA^{Trp} (Figure S1F). These results clearly demonstrate that Cdk5rap1 is a two [4Fe-4S] cluster-containing mitochondrial methylthiotransferase that specifically converts i⁶A to ms²i⁶A at A37 of mt-tRNA^{Phe}, mt-tRNA^{Trp}, mt-tRNA^{Tyr}, and mt-tRNA^{Ser(UCN)} in mammalian cells.

The ms² Modification Controls Codon-Specific Decoding Fidelity in a Translation Rate-Dependent Manner

A previous study demonstrated that the ms² group of 2-methylthio-*N*⁶-hydroxyisopentenyl adenosine (ms²io⁶A) is critical for the accurate decoding of Tyr and Phe codons (Urbonavicius et al., 2001). To thoroughly investigate the role of ms² modifications of tRNAs during the decoding of their cognate codons, we utilized a luciferase-based reporter and transformed the plasmid into a WT strain or the Δ MiaB strain to detect frameshifting in the presence or absence of the ms² modification. The firefly luciferase gene was properly translated only when frameshifting occurred at the cognate codons read by tRNA^{Phe}, tRNA^{Trp}, tRNA^{Tyr}, or tRNA^{Ser(UCN)} (Figure S2E). A deficiency in ms² modification induced frameshifting at Phe(TTT) and Tyr(TAT) codons (Figure 1G). Induction of protein translation by isopropyl-beta-D-thiogalactopyranoside (IPTG) exaggerated the overall frameshifting rate in both the WT and Δ MiaB strains. In addition to the Phe(TTT) and Tyr(TAT) codons, there was a significant increase in ms²-dependent frameshifting at the Tyr(TAC), Ser(TCT), Ser(TCC), and Ser(TCG) codons, for which frameshifting was not observed without IPTG induction (Figures S1G–S1I). Importantly, these results show that ms²-dependent frameshifting specifically occurred during the translation of wobble codons, such as Phe(TTT), Tyr(TAT), Ser(TCT), Ser(TCC), and Ser(TCG), with the exception of the Tyr(TAC) codon, but not the cognate codons, such as Phe(TTC), Ser(TCA), and Trp(TGG) (shown in red in Figures S1F–S1I). Furthermore, the ms²-deficiency-evoked frameshifting was fully reversed by transformation with active Cdk5rap1, but not dominant-negative Cdk5rap1 (Figure 1G). These results demonstrate that ms² modification is critical for the accurate decoding of wobble codons corresponding to tRNA^{Phe}, tRNA^{Tyr}, or tRNA^{Ser(UCN)} in a translation rate-dependent manner.

Deficiency of the Mitochondrial ms² Modification Attenuates Mitochondrial Translation

To examine mitochondrial protein synthesis, WT or KO MEF cells were labeled with ³⁵S-methionine for 1 hr and subjected to pulse chase. The mitochondrial protein synthesis was substantially decreased in KO MEF cells (Figure 2A). Furthermore, MEF cells were radioactively labeled and subjected to blue native PAGE to examine the formation of respiratory complexes. The incorporation of mitochondrial proteins into complexes I, III, and IV was substantially decreased in KO MEF, whereas complex V was unaffected (Figures 2B and 2C). These results suggest that the deficiency in ms² modification greatly attenuated mitochondrial protein synthesis, resulting in impaired complex assembly.

The maintenance of mitochondrial OXPHOS subunits is critical for the electron transport chain, which maintains the resting

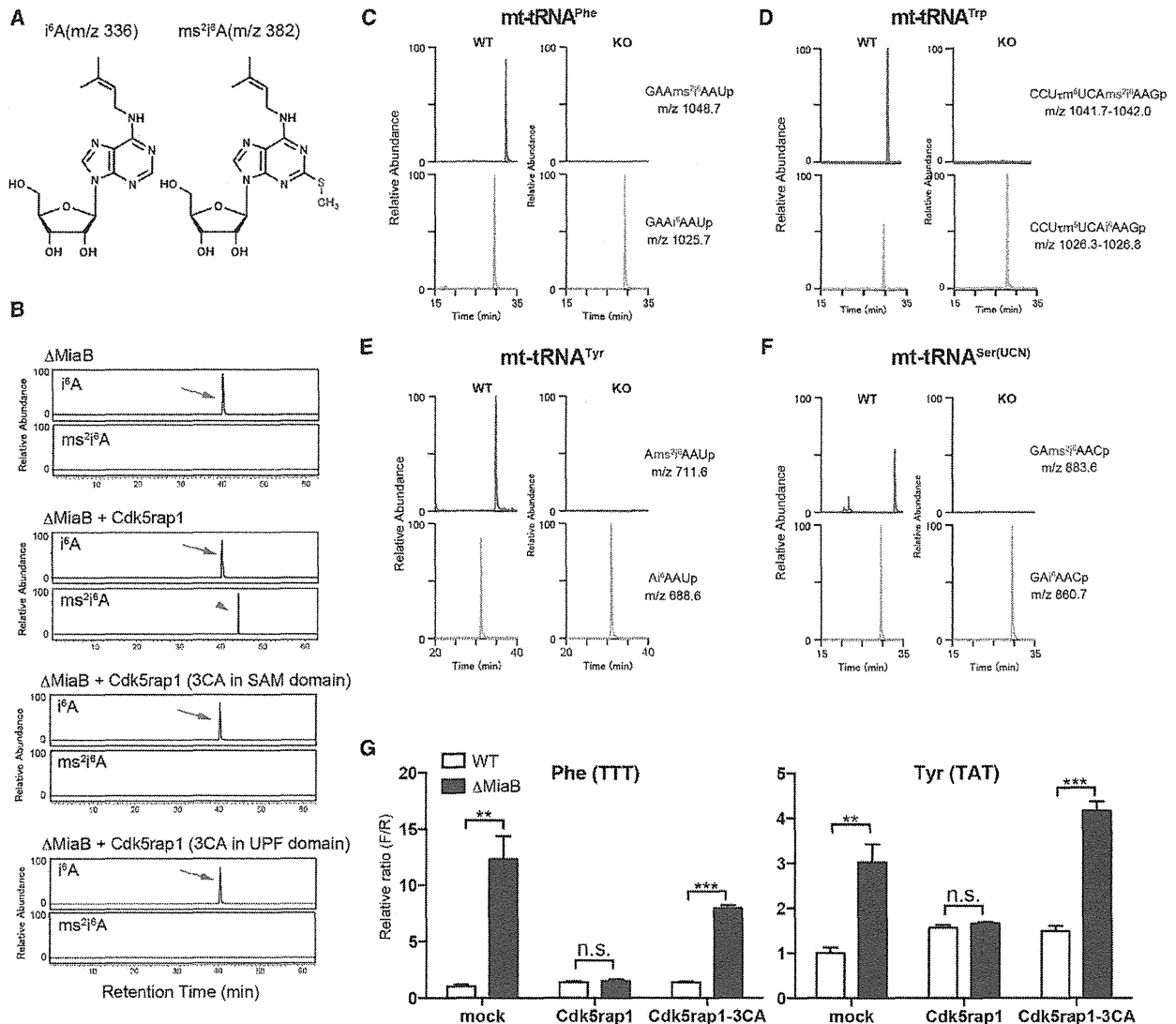


Figure 1. Cdk5rap1 is The Mammalian mt-tRNA Methylthiotransferase

(A) Structures of N⁶-isopentenyladenosine (i⁶A) and 2-methylthio-N⁶-isopentenyladenosine (ms²i⁶A) and the corresponding m/z values are shown. The ms² group (S-CH₃) is shown in red.

(B) GST-Cdk5rap1 or GST-Cdk5rap1 with Cys-to-Ala mutations (3CA) was transformed into the MiaB-deficient strain (ΔMiaB). The arrows and arrowhead indicate the peaks corresponding to i⁶A and ms²i⁶A, respectively.

(C–F) Examination of the ms²i⁶A modification in mt-tRNA^{Phe} (C), mt-tRNA^{Trp} (D), mt-tRNA^{Tyr} (E), and mt-tRNA^{Ser(UCN)} (F) isolated from WT and KO mice by mass spectrometry. The mass chromatograms show the peaks corresponding to fragments containing i⁶A or ms²i⁶A.

(G) Frameshift assay. WT and ΔMiaB bacteria were transformed with Cdk5rap1 or inactive Cdk5rap1 (Cdk5rap1-3CA). The relative ratio of firefly luciferase activity to renilla luciferase activity (F/R) represents the decoding error. n = 4. Data are mean ± SEM. **p < 0.01, ***p < 0.0001.

mitochondrial membrane potential and drives respiration. We thus investigated the mitochondrial membrane potential in WT and KO MEF cells. There was a marked increase in cell populations with very low membrane potential in KO MEF cells (Figure 2D). Consequently, the oxygen consumption rate in KO cells was significantly lower than that in WT MEF cells (Figure 2E). Furthermore, the KO cells quickly lost their mitochondrial membrane potential after treatment with very low doses of rotenone and FCCP, which had little effect on WT cells (Figures 2F and

2G). These results thus demonstrate that ms² modifications of mt-tRNAs are critical for maintaining efficient mitochondrial translation and respiratory chain.

Deficiency of Mitochondrial ms² Modification Impairs OXPHOS in Skeletal Muscle and Heart Tissue without Affecting Basal Metabolism

To investigate the physiological role of mitochondrial ms² modification, we examined the phenotype of KO mice in vivo. Despite

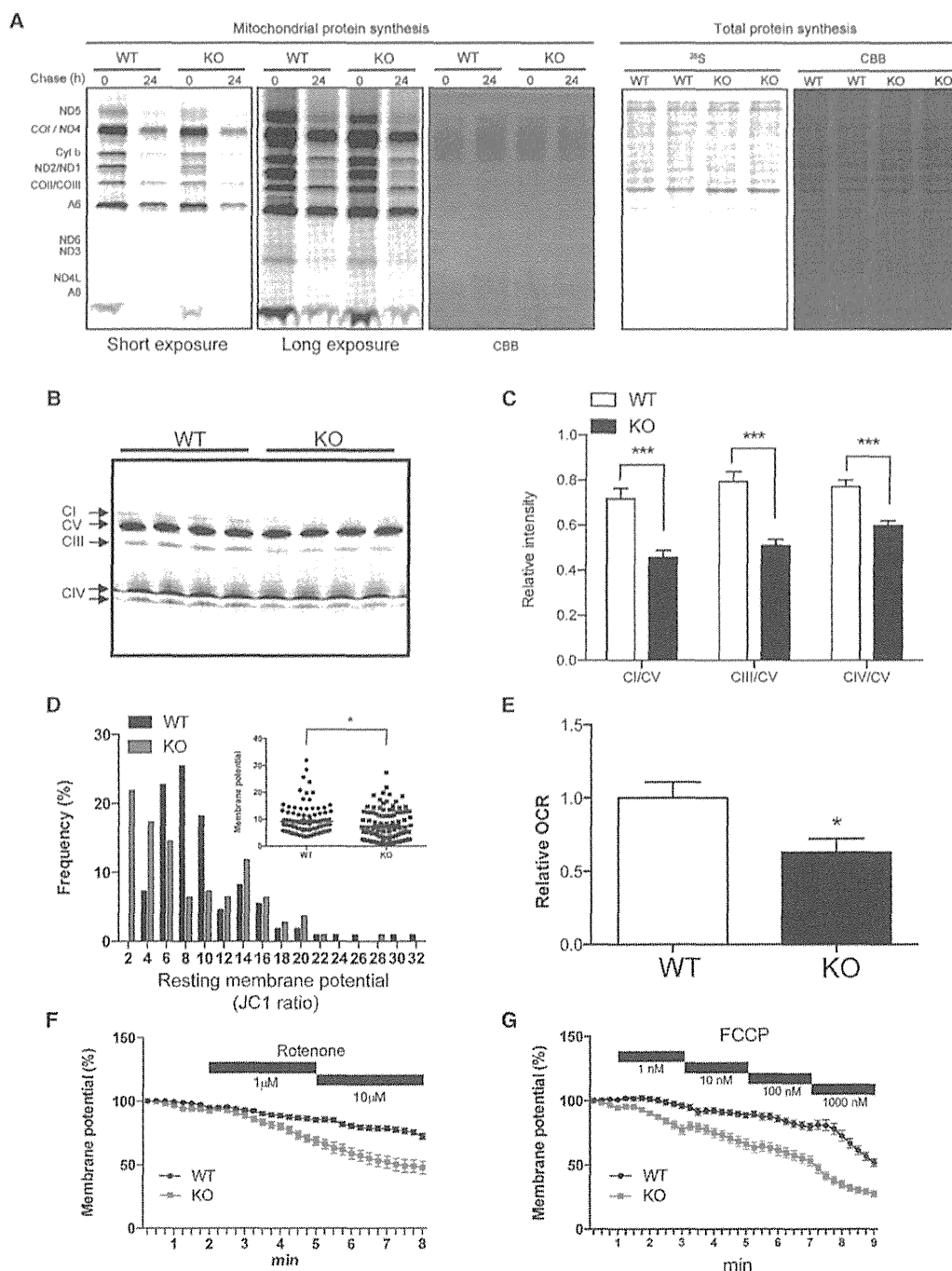


Figure 2. Deficiency in the ms^2 Modifications impaired Mitochondrial Protein Synthesis and Mitochondrial Functions

(A) WT and KO MEF cells were labeled with ³⁵S-Met/Cys and chased for 0 or 24 hr in the presence of emetine for measurement of mitochondrial protein synthesis (left panels). MEF cells were labeled with ³⁵S-Met/Cys for 1 hr, and total protein synthesis was measured (right panels). CBB staining of gel was used as loading control.

(B and C) The autoradiogram of blue native PAGE shows a decrease in the incorporation of mitochondrial proteins in complexes I, III, and IV in KO MEF cells (B). The relative intensity of complex I, III, and IV versus complex V was quantified (C).

(D) The histogram and inserted graph show that KO MEF cells contain a number of mitochondria with low membrane potentials; n = 110 each.

(E) KO cells showed a significant decrease in the oxygen consumption rate (OCR); n = 10 each.

(E–G) Cells were stained with TMRM for measuring membrane potential. The relative membrane potential in the presence of rotenone (F) or FCCP (G) was analyzed; n = 66 for WT and n = 30 for KO (F); n = 43 for WT and n = 32 for KO (G). Data are mean ± SEM. *p < 0.05.

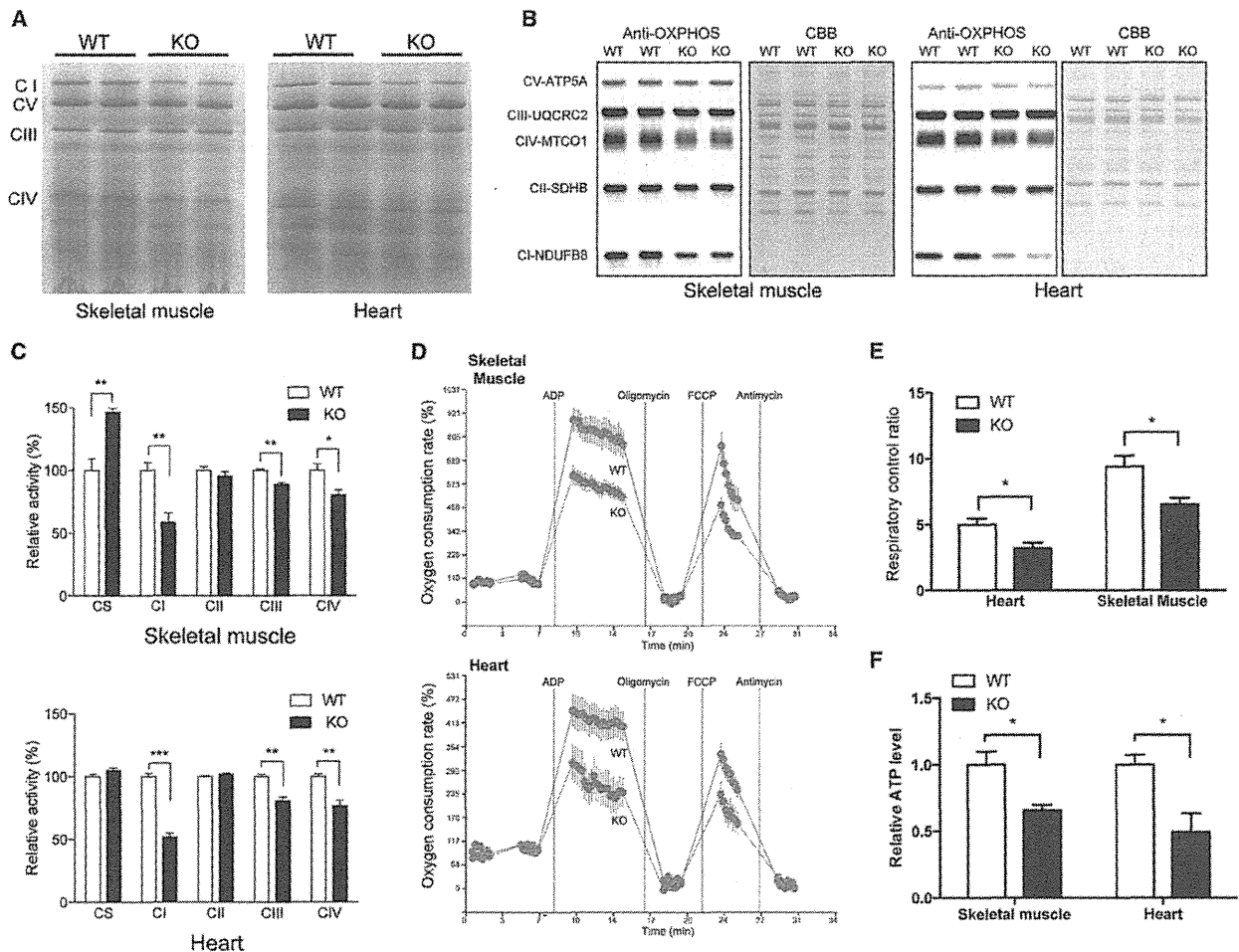


Figure 3. The Deficiency in m^2 Modification Impaired Mitochondrial Function in Vivo

(A) Steady-state levels of complex I (CI), complex II (CII), complex III (CIII), complex IV (CIV), and complex V (CV) in mitochondria isolated from skeletal muscle and heart tissues were examined by BN-PAGE.

(B) Steady-state levels of representative proteins of CI–CIV were examined by western blotting. CBB staining was used as loading control.

(C) The activities of CS, CI–CIV in skeletal muscle (left panel), and heart (right panel) of WT and KO mice were examined. $n = 4–5$.

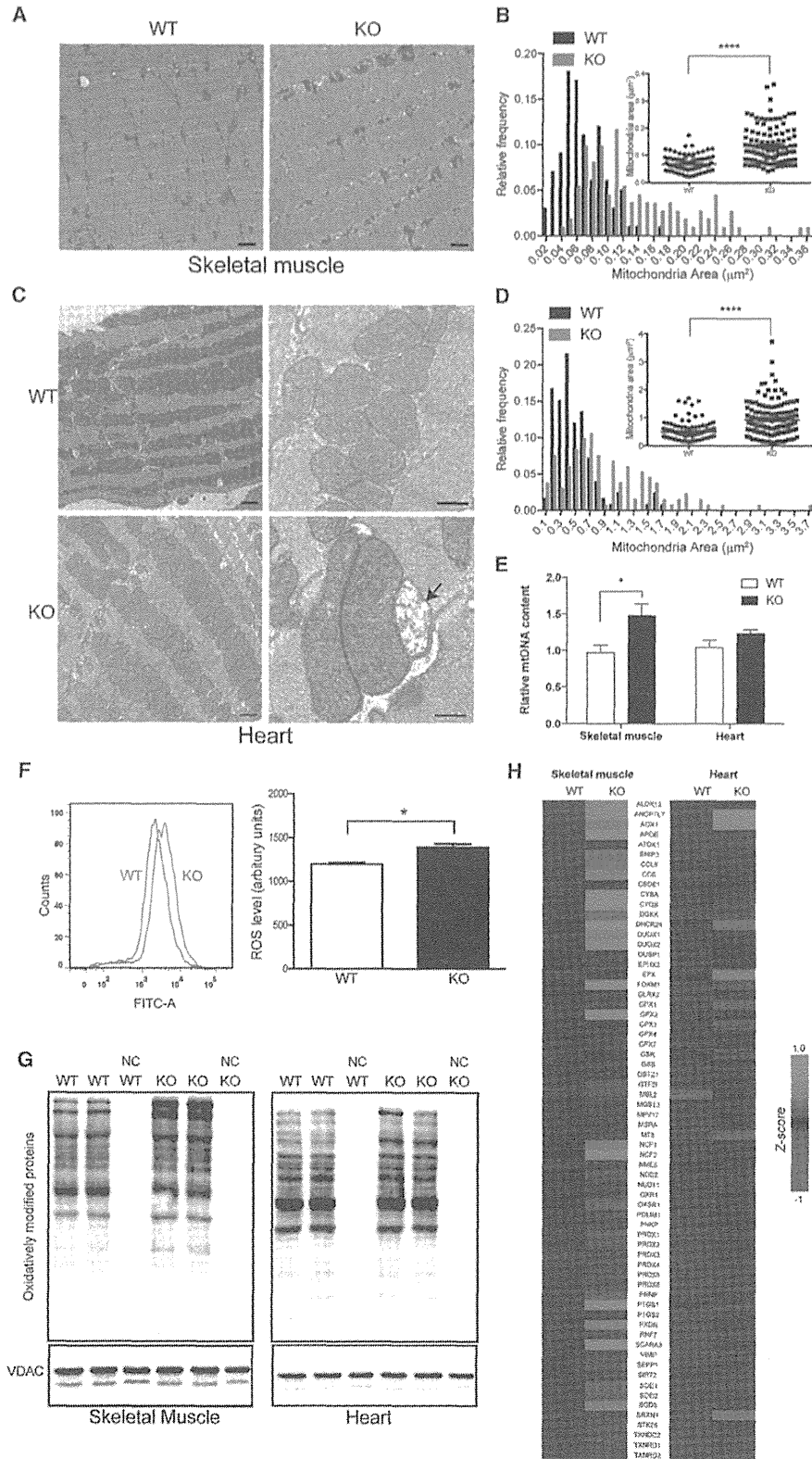
(D and E) Respiratory coupling was decreased in *Cdk5rap1*-deficient mitochondria isolated from skeletal muscle and heart tissue when examined using XF24 Flux Analyzer; $n = 4–5$.

(F) The steady-state levels of ATP in the skeletal muscle and heart tissue of WT and KO mice were examined; $n = 4$ each. Data are mean \pm SEM. $*p < 0.05$.

the mitochondrial dysfunction in KO cells, the *Cdk5rap1* KO mice developed normally without obvious morphological changes in major tissues (Figures S3A and S3B). The energy expenditure and glucose metabolism in KO mice were compatible with those of WT mice (Figures S3C–S3E). Furthermore, there was no difference in neurological behaviors between KO and WT mice (Figures S3F–S3I).

Of all tissues, skeletal muscle and heart tissue are the most susceptible tissues to mitochondrial dysfunction (DiMauro and Schon, 2003). We therefore closely examined these two tissues in KO mice. Substantial decreases in the steady-state levels of complex I and IV were observed in both skeletal muscle and heart tissues of KO mice compared with WT mice, with complex I being markedly affected (Figure 3A). Accordingly, the steady-state levels of complex I and IV proteins, such as NDUFB8 and

MTCO1, respectively, were markedly decreased in skeletal muscle and heart tissues of KO mice compared with WT mice (Figure 3B). As a result, complex I activity was significantly impaired in KO mice (58.6% of WT for skeletal muscle and 51.5% of WT for heart tissue) (Figure 3C). There was a mild but significant decrease in complex III and complex IV activity in KO mice (muscle: complex III, 88.8% of WT; complex IV, 80.5% of WT; heart: complex III, 80.7% of WT, complex IV, 79.8% of WT) (Figure 3C). The decrease in mitochondrial activity in the skeletal muscle of KO mice was also confirmed by cytochrome oxidase (COX) staining (Figure S3J). Accordingly, the oxygen consumption elicited by ADP and FCCP in *Cdk5rap1*-deficient mitochondria was significantly lower than that in WT mitochondria, indicating that electron transport and respiratory coupling were impaired in the skeletal muscle and heart tissue of KO mice (respiratory



(legend on next page)

control ratio of the hearts of WT and KO: 4.9 and 3.2, skeletal muscles of WT and KO: 9.4 and 6.5, respectively; Figures 3D and 3E). Consequently, the steady-state ATP level in skeletal muscle and heart tissue of KO mice was lower than that in WT mice (Figure 3F).

Impairment of mitochondrial function usually exaggerates mitochondrial remodeling as a compensation mechanism. There was an increase in the mitochondrial mass in the skeletal muscle of KO mice as examined by electron microscopy and Gomori Trichrome staining (Figures 4A, 4B, and S3J). Strikingly, the mitochondria were abnormally enlarged in heart tissue of KO mice (Figures 4C and 4D). A progressive disruption of cristae was occasionally observed in the mitochondria of the cardiac muscle of KO mice (arrow in Figure 4C). Furthermore, there was a significant increase in citrate synthase activity (Figure 3C) as well as relative mtDNA content (Figure 4E) in the skeletal muscle of KO mice.

Reactive oxygen species (ROS) are byproducts of mitochondrial electron transport and mainly generated from complexes I and III (Murphy, 2009). A deficiency of complexes I and III accelerates the leakage of ROS from electron transport chain and contributes to the development of mitochondrial diseases. Given the marked decrease in complex I protein level in KO mice, we investigated ROS production in KO mice (Figure 4F). The ROS level was slightly but significantly higher in KO MEF cells than that in WT MEF cells. This finding was corroborated by a moderate increase in protein carbonylation (Figure 4G) as well as oxidative stress-related gene expression in both skeletal muscle and heart tissues of KO mice (Figure 4H).

To further investigate the impact of deficiency of ms^2 modification on physiological function, we examined muscular and cardiac function in vivo. However, the treadmill performance of KO mice was comparable with that of WT mice (Figure S3K). The echocardiography examination indicated that no apparent cardiac defects were present in the KO mice (Figure S3L). Taken together, these results demonstrate that the deficiency of ms^2 modifications in mt-tRNAs impairs mitochondrial protein synthesis, which leads to a reduction of respiratory activity and increase in ROS in skeletal muscle and heart tissue. However, considering the overall phenotypes, mice seem to tolerate an up to 50% reduction of complex I activity due to the loss of ms^2 modifications under sedentary conditions.

Loss of ms^2 Modifications Accelerates OXPHOS Defects under Stressed Conditions

The mild phenotype of KO mice prompted us to challenge the mice with a ketogenic diet (KD; very high fat and ultra-low carbohydrate). Ketone bodies from KD bypass glycolysis and generate

energy mostly through fatty acid oxidation in mitochondria (Lafel, 1999). Adaptation to this metabolic pressure is accompanied by mitochondrial rearrangement (Grimsrud et al., 2012). Therefore, it is conceivable that the accurate regulation of mitochondrial protein synthesis by ms^2 modification is particularly important for mitochondrial remodeling under stressed conditions.

As expected, KD treatment accelerated OXPHOS defects in the skeletal muscle and heart tissue of KO mice (Figures 4A and 4B). Complex I activity was significantly impaired in KD-fed KO mice (48.6% of the KD-fed WT for skeletal muscle and 47.7% of the KD-fed WT for heart tissue) (Figures 5A and 5B). In addition, accelerated decreases in complex III and IV activities were observed in the KD-fed KO mice (muscle: complex III, 82.9% of the KD-fed WT; complex IV, 62.9% of the KD-fed WT; heart: complex III, 75% of the KD-fed WT; complex IV, 57.8% of the KD-fed WT).

The OXPHOS defect after KD treatment exaggerated the mitochondrial remodeling pathway in both WT and KO mice. There was a ~ 3 -fold and ~ 1.5 -fold increase in mtDNA content in the skeletal muscle and heart tissue of both WT and KO mice fed a KD, respectively (Figure 5C). However, there was no difference in the mtDNA content in skeletal muscle and heart tissue between WT and KO mice (Figure 5C). Accordingly, subsequent electron microscopic examination revealed a marked increase in mitochondria mass (Figures 5D and 5F). In the skeletal muscles of KO mice fed a KD, mitochondrial proliferation was observed in both intermyofibrillar and subsarcolemmal mitochondria, with the latter drastically increased (Figure 5D). Importantly, KD-fed KO mice exhibited a considerable population of mitochondria with disrupted cristae in the skeletal muscle tissue (arrowheads in Figure 5D). The enlargement of mitochondria and the disruption of cristae were even more prominent in the heart tissue of KO mice fed a KD (arrows in Figure 5D). These results demonstrate that Cdk5rap1-dependent ms^2 modification is crucial for the maintenance of OXPHOS activity and mitochondrial morphology under stress.

The acceleration of the OXPHOS defect in KO mice may be due to the indirect lipotoxicity from the very high-fat diet. However, the body weight and serum metabolic profiles of KO mice fed a KD were the same as those of WT mice fed a KD (Figures S4A–S4C). There was no difference in the locomotor activity or energy expenditure between the WT and KO mice fed a KD (Figures S4D and S4E). Interestingly, the glucose level in the KD-fed KO mice was somewhat lower than that in the KD-fed WT mice (Figure S4F). Taken together, these results indicate that the progressive OXPHOS defects and mitochondrial degeneration in KD-fed KO mice directly resulted from a deficiency in Cdk5rap1-dependent ms^2 modification during mitochondrial remodeling.

Figure 4. Aberrant Mitochondrial Morphology and ROS Metabolism in KO Mice

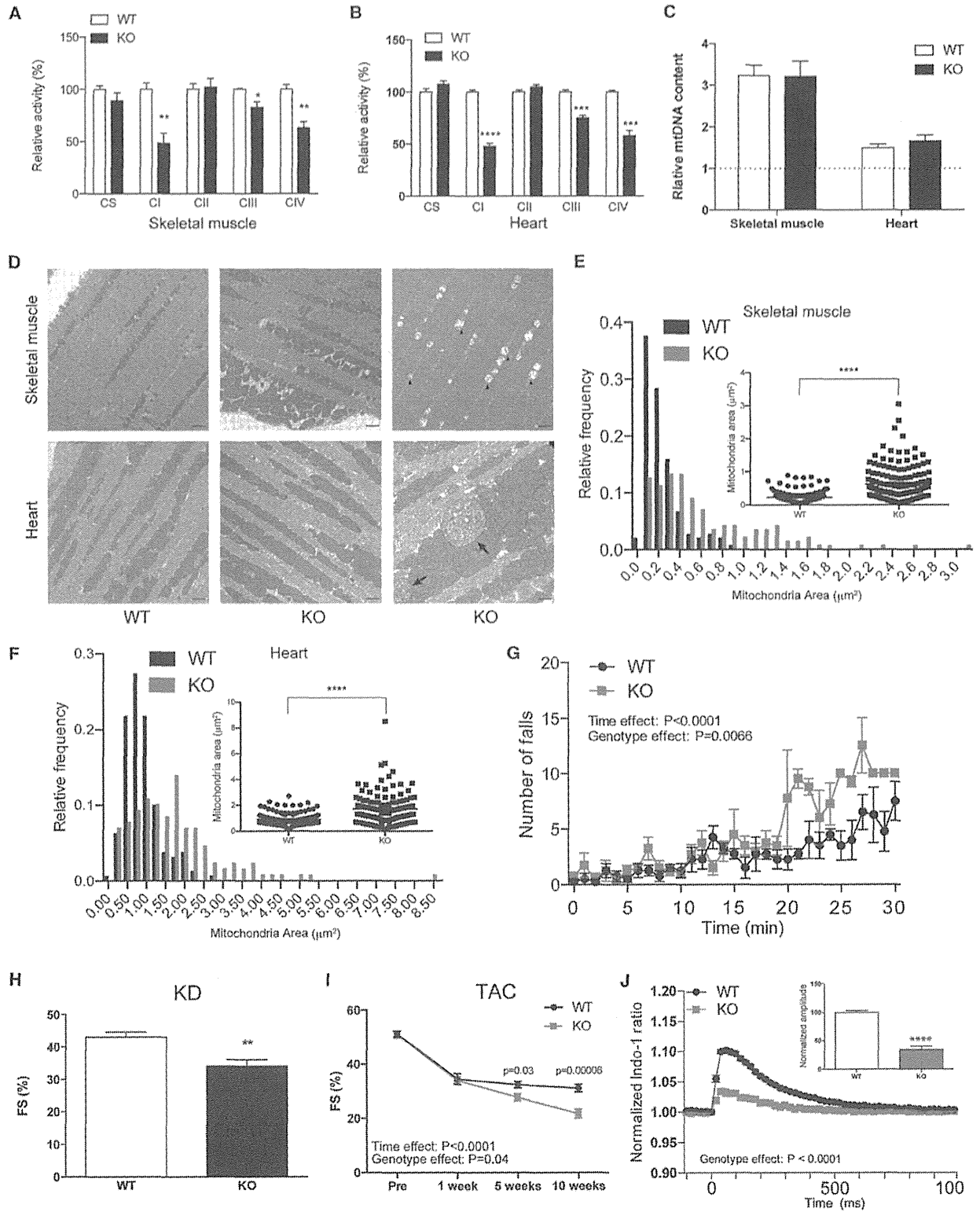
(A–D) Mitochondria in skeletal muscle and heart tissue were examined by electron microscopy. KO mice exhibit disrupted mitochondrial morphology (A and C) and increased mitochondrial mass (B and D). Bars in (A) and the left panels of (C), 10 μ m. Bars in the right panels of (C), 0.5 μ m. WT, n = 100; KO, n = 112 in (B) and n = 126; KO, n = 132 in (D).

(E) The relative contents of mtDNA in muscle and heart tissue were examined; n = 6–9.

(F) ROS levels were analyzed by measuring the fluorescent intensity of CM-H2DCFDA in WT and MEF cells (left panel). The intensity was quantified (right panel); n = 3.

(G) Protein carbonylation levels were increased in the mitochondria of skeletal muscle and heart tissue in KO mice.

(H) Heatmap showing the differentially regulated genes involved in oxidative stress response in skeletal muscle and heart tissue of WT and KO mice; n = 4. Data are mean \pm SEM. *p < 0.5, ****p < 0.0001.



(legend on next page)

Loss of ms^2 Modification Accelerates Muscular and Cardiac Dysfunction under Stress

The KD-induced OXPHOS defect markedly accelerated the dysfunction of skeletal muscle and heart tissue in the KO mice. In a treadmill test, KO mice fed a KD showed a significant increase in the number of falls and became exhausted as early as 30 min into the test (Figure 5G). The KO mice also showed moderate cardiac hypertrophy, as indicated by an increase in heart volume, heart weight, and left ventricle posterior wall thickness (Figures S5A–S5C). The percentage of fractional shortening (FS%) in KO mice fed a KD was significantly lower than that in WT mice fed a KD (WT, 43% versus KO, 34%; Figure 5H). In addition to a KD-induced stress model, we utilized a transverse aortic constriction (TAC) model, which is a standard model for inducing cardiac dysfunction by pressure overload. Because the TAC model is also accompanied by global mitochondrial remodeling (Dai et al., 2012), we expected that a deficiency in ms^2 modification would further accelerate cardiac dysfunction. Indeed, chronic TAC resulted in a progressive cardiac hypertrophy, as indicated by an increase in heart weight and left ventricle posterior wall thickness in KO mice (WT, 7.5 mg/g body weight; KO, 11.3 mg/g body weight; Figures S5A and S5D–S5F). In WT mice, the FS% dropped from 51.2% to 34.5% 1 week after TAC but was then maintained until 10 weeks (5 weeks, 32.4; 10 weeks, 31.1; Figure 5I). In contrast, the FS% in KO mice continuously decreased after TAC and eventually decreased to as low as 21.7% (Figure 5I). Further examination in isolated cardiomyocytes revealed that the cardiac dysfunction observed in the TAC model of KO mice was associated with a decrease in calcium influx and contraction rate (Figures 5J and S5G). These results demonstrate that a deficiency of the ms^2 modifications in mt-tRNAs can cause a catastrophic defect in muscle and heart tissue under stressed conditions.

Deficiencies in ms^2 Modification Compromise the Quality of Mitochondria

Next, we investigated the molecular mechanism underlying the stress-induced acceleration of OXPHOS defects and cardiomyopathy in KO mice. Adaptation to mitochondrial stress requires coordinated protein synthesis (Dai et al., 2012). Because ms^2 modification controls decoding fidelity in a translation-rate-dependent manner, it is conceivable that a deficiency in ms^2 modification under stressed conditions might markedly compro-

mise mitochondrial quality as well as integrity, which would result in severe OXPHOS defects and ultimately lead to myopathy and cardiac dysfunction. Indeed, a moderate increase in the complex I level was observed in WT mice treated with KD or TAC surgery (Figures 6A and 6B). In contrast, the steady-state levels of complexes I and IV levels were somewhat decreased in KD-fed and TAC KO mice when compared with NC-fed KO mice. The mitochondrial stresses increased protein carbonylation in both WT and KO mice. As a result, the protein carbonylation level in stressed heart tissues of KO mice was moderately higher than that in the stressed WT mice (Figure S6A). Impaired mitochondrial proteostasis exaggerates mitochondrial unfolded protein response (mt-UPR) (Durieux et al., 2011; Houtkooper et al., 2013). Accordingly, proteins involved in mtUPR, such as Yme11, Afg3l2, and Lonp1, were upregulated in mitochondria isolated from the hearts of KO mice treated with KD and TAC compared with WT mice (Figure 6C). Furthermore, a marked increase in polyubiquitinated proteins was observed in mitochondria isolated from the hearts of KO mice under stressed conditions (Figure 6D). Interestingly, the levels of polyubiquitination were proportional to the levels of cardiac function (FS%) in stressed KO mice (TAC > KD > NC; Figure 6D; also see Figures 5H and 5I).

Mitophagy is the hallmark of the existence of compromised mitochondria. Parkin, an E3 ubiquitin ligase, primes mitophagy by translocation to mitochondria with low membrane potentials and ubiquitination of mitochondrial proteins (Kubli and Gustafsson, 2012). Because cells with ms^2 modification deficiencies had a low basal mitochondrial membrane potential and were susceptible to stress-induced depolarization (Figures 2F and 2G), we hypothesized that mitochondrial stress might exaggerate the recruitment of Parkin to mitochondria and the acceleration of mitophagy in Cdk5rap1 KO cells. In KO cells treated with FCCP, most of the Parkin translocated to the mitochondria as soon as 2 hr after treatment, whereas similar translocation was not observed in WT cells treated with FCCP (Figure 6E; also see the separated imaged in Figure S6B). A number of large mitochondrial aggregates were surrounded by the autophagosomal membrane protein LC3 in KO cells treated with FCCP, which is indicative of acceleration of mitophagy (Figure 6F; also see the separated imaged in Figure S6C). Furthermore, we observed a number of degenerated mitochondria, with some mitochondria being degraded in autophagic vacuoles in KD-fed and TAC KO mice, by electron microscopic examination (Figure 6G). These

Figure 5. Mitochondrial Stresses Accelerated Myopathy and Cardiac Dysfunction in ms^2 -Deficient Mice

(A and B) WT and KO mice at 8 weeks old were fed for KD for 10 weeks. The relative activities of CS, CI-CIV in skeletal muscle (A), and heart (B) were examined; n = 5–7 each.

(C) The relative mtDNA contents in skeletal muscle and heart tissue of KD-fed WT and KO mice were examined; n = 6–7. The dashed lines represent the relative mtDNA content in NC-fed WT mice.

(D–F) Electron microscopy examination of skeletal muscle and heart tissue show disrupted mitochondrial architecture (D) and a marked increase in mitochondrial mass (E and F) in KD-fed KO mice. Arrowheads and arrows indicate mitochondria with abnormal cristae in skeletal muscle and heart tissues of KD-fed KO mice, respectively; bars, 10 μ m; WT, n = 152; KO, n = 144 in (E) and n = 161; KO, n = 130 in (F).

(G) A treadmill test performed at the end of 10 weeks of KD feeding showed that the KD induced a higher number of falls in the KO mice during acute exercise compared with the WT mice; n = 5 each.

(H) The fractional shortening (FS) rate in KO mice fed with KD for 10 weeks was significantly lower than that in KO-fed WT mice; n = 10–11.

(I) WT and KO mice at 8 weeks old were subject to TAC surgery. The KO mice showed a significant decrease in FS after TAC surgery.

(J) Cardiomyocytes were isolated from WT and KO mice 10 weeks after TAC. Calcium imaging revealed a decrease in the peak calcium influx in KO cardiomyocytes. The inserted graph shows the normalized peak amplitude of calcium influx in cardiomyocytes from WT and KO mice; n = 13 for WT and n = 6 for KO. Data are the mean \pm SEM. *p < 0.05. **p < 0.01, ***p < 0.001, ****p < 0.0001.